Supplementary Information

Structure of human mitochondrial RNA polymerase elongation complex

Kathrin Schwinghammer[1], Alan C.M. Cheung[1], Yaroslav I. Morozov[2], Karen Agaronyan[2], Dmitry Temiakov[2] and Patrick Cramer[1]

[1]Gene Center and Department of Biochemistry, Ludwig-Maximilians-Universität München, Munich, Germany.

[2]Department of Cell Biology, School of Osteopathic Medicine, Rowan University, Stratford, New Jersey, USA.

Supplementary Information comprises:

Supplementary Figures 1–5

Supplementary Tables 1–2

Supplementary Video 1

Nature Structural and Molecular Biology: doi:10.1038/nsmb.2683

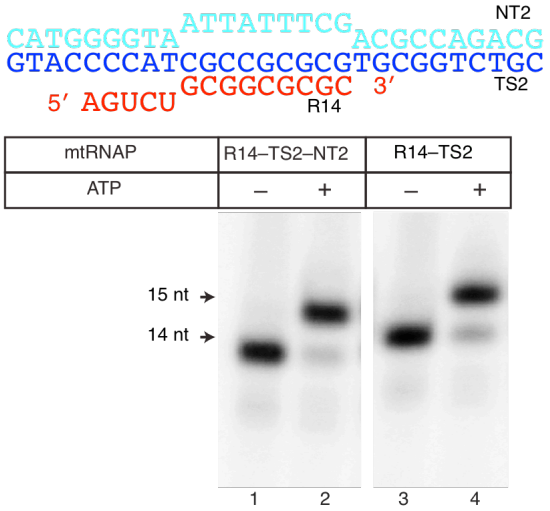

Supplementary Figure 1 Activity of mtRNAP elongation complex assembled on nucleic acid scaffolds.

mtRNAP (1 mM) was pre-incubated with the scaffolds indicated (1 mM) for 5 min at room temperature and the ^{32}P-labeled RNA primer extended by addition of 10 mM of adenosine triphosphate (ATP) for 2 min. The products of the reaction were resolved in 20% PAGE containing 6 M urea.

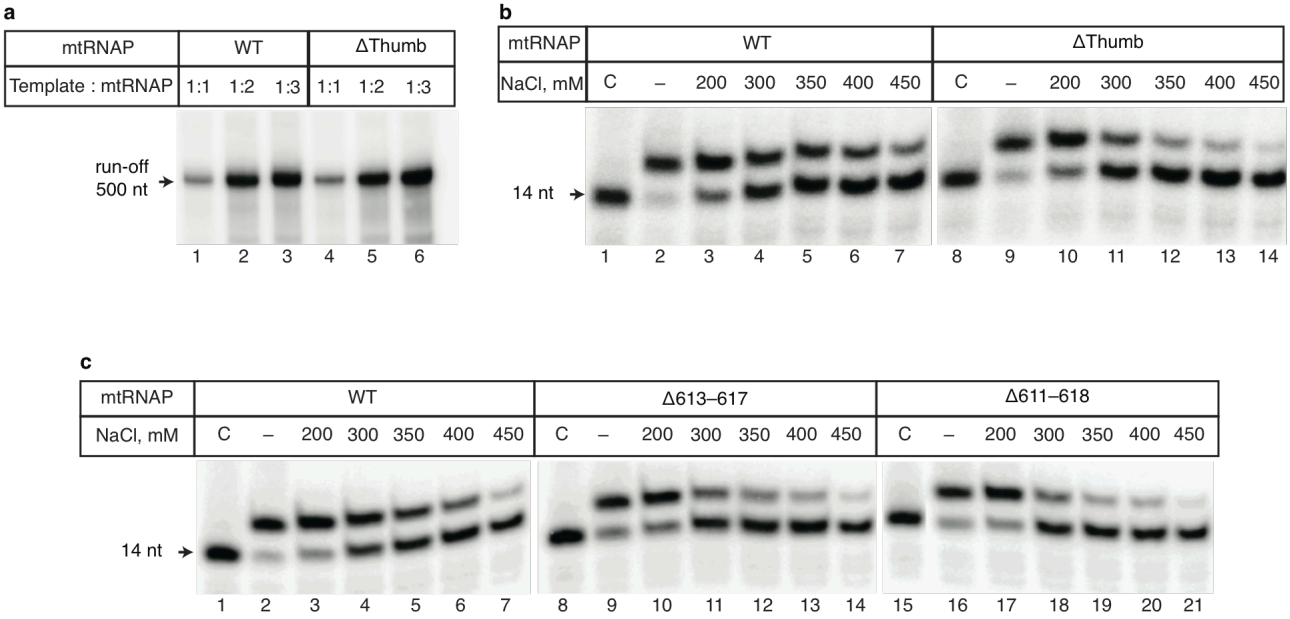

Supplementary Figure 2 Effects of mtRNAP variants on elongation complex stability.

(a,b) Thumb deletion mtRNAP mutant is processive but forms unstable halted elongation complexes. **(a)** Processivity of the Δthumb mtRNAP. Run-off transcription assay was performed using PCR template containing the LSP promoter (50 nM) and the indicated amount of WT (lanes 1–3) and Δthumb (lanes 4–6) mtRNAPs and the products of the reactions resolved in 20% PAGE containing 6 M urea. **(b)** ΔThumb mutant forms an unstable halted elongation complex. The elongation complexes were assembled using R14–TS2–NT2 scaffold and WT or Δthumb mtRNAP. As a control (C) only polymerase was loaded in lanes 1 and 8.

(c) Elongation complexes formed with mtRNAP variants that contain a deletion of the intercalating hairpin are sensitive to salt challenge. Elongation complexes were formed using R14–TS2–NT2 scaffold and WT (lanes 1–7) or the intercalating hairpin deletion mutants Δ613–617 (lanes 8–14) and Δ611–618 (lanes 15–21). As a control (C) only polymerase was loaded in lanes 1,8 and 15.

Nature Structural and Molecular Biology: doi:10.1038/nsmb.2683

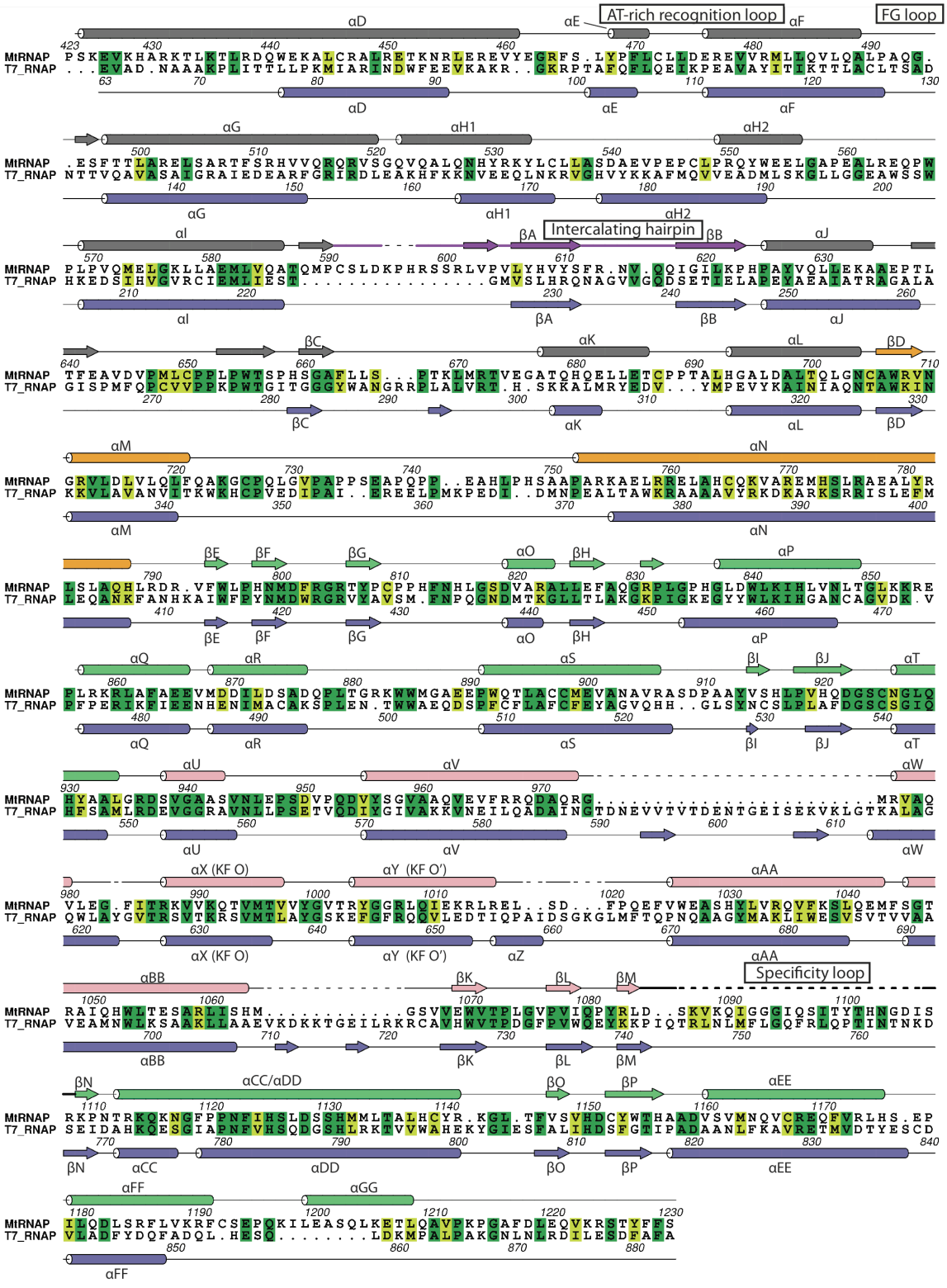

Supplementary Figure 3 Structure-based sequence alignment and conservation of human mtRNAP (residues 423–1230) and T7 RNAP (residues 63–883, PDB 1QLN).

Secondary structure elements are consecutively labeled in alphabetical order (cylinders, α-helices; arrows, β-strands; lines, loops). Since helix X is commonly named helix O based on a corresponding helix in the *Escherichia coli* Klenow (KF) fragment[41], we maintain this convention during this work. Identical residues are highlighted in dark green, conservative substitutions are shown light green. Color coding for mtRNAP secondary elements is as in **Figs. 1–3**.

Nature Structural and Molecular Biology: doi:10.1038/nsmb.2683

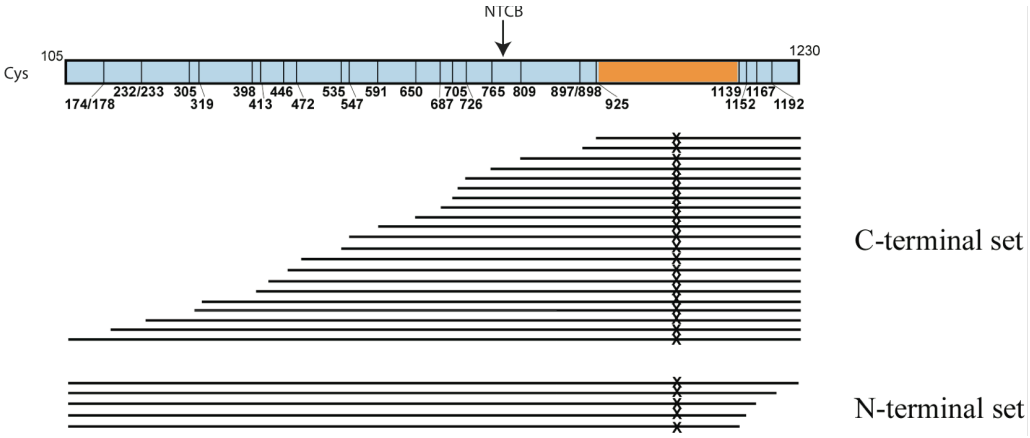

Supplementary Figure 4 Analysis of cross-linking mapping data.

Cross-linking mapping with NTCB and CNBr (**Fig. 4a**) was performed using the so-called "single-hit" conditions[42,43] i.e. when every mtRNAP molecule is cleaved only once, on average. Thus, the single-hit conditions generate characteristic patterns of the N-terminal and C-terminal cleavage products. As an example, the theoretical pattern of mtRNAP cleavage by NTCB consistent with the position of the cross-link at the C-terminus is presented above. The size of the labeled fragments is identified by its mass (mobility in SDS PAGE) using SeeBlue protein standard markers (Invitrogen). To distinguish between the C-terminal and the N-terminal location of the cross-link two variants of mtRNAP were used, WT mtRNAP and Δ104 mtRNAP (**Fig. 4a**). No shift in bands migration was observed in SDS-PAGE (**Fig. 4a,** lanes 2 and 3) confirming the location of the cross-link site at the C-terminus of mtRNAP. The smallest labeled band visible on the SDS PAGE upon NTCB treatment corresponds to the 925–1230 peptide and thus positions the cross-linking site between residues C925 and C1139. This interval was narrowed down even further by CNBr cleavage (**Fig. 4a,** lanes 5 and 6). The smallest band visible on the gel upon CNBr treatment corresponds to the 1064–1230 peptide and positions the cross-linking site between residues M1063 and M1132.

Cross-linking mapping of RNA at base –13 was perfomed using mtRNAP variants having a single hydroxylamin clevage site (NG pair) at a defined position (**Fig. 4b**). The cleavage generates only two mtRNAP fragments simplifying identification of the labeled peptides. Thus the cleavage of the cross-link obtained with NG493 mutant

results in apperance of a labeled fragment (83.2 kDa) representing the C-terminus of mtRNAP, while cleavage of NG634 mutant results in appereance of the N-terminal fragment (61.5 kDa). Taken together, these data suggest that the cross-linking site is between residues 494 and 634.

Mapping of cross-link at DNA template base at –8 (**Fig. 4c**) was perfomed using NH_2OH and WT, NG556 and NG634 mtRNAPs. WT mtRNAP contains four sites for NH_2OH clevage at positions 710, 926, 1103 and 1117, however the most N-terminal site (710) is cleaved inefficiently and thus the resulting peptides are not visible. NH_2OH clevage of the mtRNAP-DNA cross-link results in two major products corresponding to the intervals 44–926 and 44–1103 or 44–1117 (**Fig. 4c,** lane 6). Since no band was oserved that corresponds to the interval 926–1103 or 926–1117 (about 28 kDa for peptide with the cross-linked DNA) we conclude that the cross-link is to the 44–926 interval of mtRNAP. Cleavage of the NG556 mutant results in appereance of the labeled C-terminal fragment (around 82 kDa), while cleavage of NG634 mutant generates two labeled fragments representing both the C- and the N-terminal parts of mtRNAP (**Fig. 4c,** lanes 1–4). Taken togehter these data suggest that the cross-link site of –8 base of DNA includes two adjacent mtRNAP regions: 557–634 and 635–926.

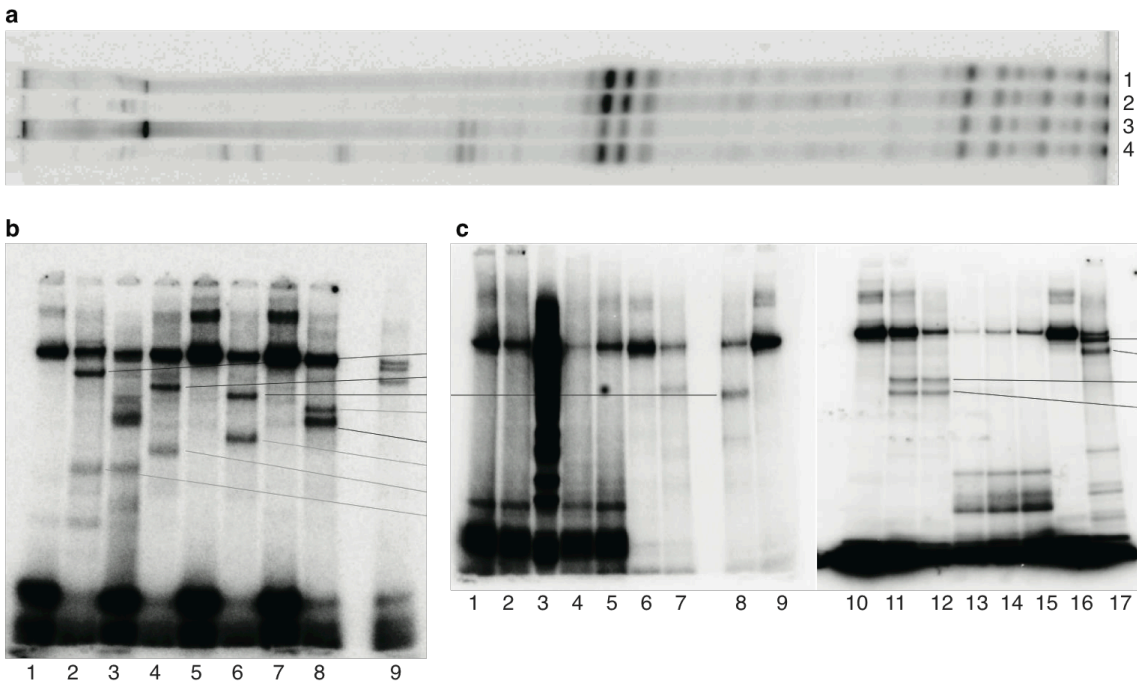

Supplementary Figure 5 Uncropped autoradiographs.
(a) Autoradiograph of transcription run-off asssays, lanes 1–4 were used to prepare **Fig. 3d**.
(b–c) Autoradiograph of cross-linking experiments. **(b)** lanes 1,2,4,6,8 were used to prepare **Fig. 4b**, **(c)** lanes 16,7,10,11,16,17 were used to prepare **Fig. 4c**.

Supplementary Table 1 Base pair parameters of mtRNAP elongation complex DNA-RNA hybrid region.

Register	Base pair	Shear (Å)	Stretch (Å)	Stagger (Å)	Buckle (°)	Propeller (°)	Opening (°)
+1	G–C	–0.57	–0.13	–0.28	–13.85	–11.09	4.34
–1	C–G	–0.12	–0.23	0.43	–2.82	–11.09	–2.26
–2	G–C	0.01	–0.22	0.14	–8.82	–9.62	–2.76
–3	G–C	–0.3	–0.13	–0.19	–9.93	–16.22	2.08
–4	C–G	0.46	–0.18	0.02	–0.39	–11.15	0.54
–5	G–C	–0.06	–0.16	–0.02	–1.93	–12.26	–1.6
–6	C–G	0.24	–0.16	0.21	–0.48	–15.32	3
–7	G–C	–0.5	–0.1	–0.28	–21.38	–11.28	2.03
–8	C–G	–0.13	–0.13	0.18	–10.77	0.16	–2.17

Register	Step	Shift (Å)	Slide (Å)	Rise (Å)	Tilt (°)	Roll (°)	Twist (°)
+1/–1	GC/GC	–0.47	–0.48	3.16	–7.74	–0.55	32.53
–1/–2	CG/CG	0.4	–1.53	3.27	4.4	6.94	33.32
–2/–3	GG/CC	0.16	–1.18	3.31	3.38	11.58	32.11
–3/–4	GC/GC	0.47	–1.14	3.08	–1.28	7.37	29.52
–4/–5	CG/CG	–0.08	–1.85	3.3	–0.65	9.86	27.91
–5/–6	GC/GC	0.24	–1.69	3.24	–1.05	4.83	29.64
–6/–7	CG/CG	0.57	–1.16	3.65	9.92	10.14	35.42
–7/–8	GC/GC	–0.15	–0.64	3.16	–2.61	13.59	28.98

Supplementary Table 2 Structural comparison of mtRNAP elongation complex NTD with different T7 NTD complexes by Cα root-mean-square deviation (RMSD) values. Structures were aligned based on the sequence alignment (**Supplementary Fig. 3**) and the RMSD calculated over all matching Cα pairs.

mtRNAP elongation complex NTD (residues 426–638) superimposed with:	RMSD (Å)
T7 initiation structure (PDB 1QLN[44], residues 72–261)	6.4
T7 initiation–elongation intermediate (PDB 3E2E[45], residues 73–254)	4.7
T7 pre–translocated product structure (PDB 1S77 (ref. 46), residues 63–261)	8.3
T7 post–translocated structure (PDB 1MSW[47], residues 63–261)	8.0

Supplemenary Video 1. Animation of the structural rearrangements between apo mtRNAP (PDB 3SPA) and its elongation complex.
The movie was generated using the morphing function of UCSF Chimera[48].

Nature Structural and Molecular Biology: doi:10.1038/nsmb.2683

Supplementary references

41 Beese, L. S., Derbyshire, V. & Steitz, T. A. Structure of DNA polymerase I Klenow fragment bound to duplex DNA. *Science* **260**, 352-355 (1993).

42 Grachev, M. A. *et al.* Studies of the functional topography of Escherichia coli RNA polymerase. A method for localization of the sites of affinity labelling. *Eur J Biochem* **180**, 577-585 (1989).

43 Korzheva, N. *et al.* A structural model of transcription elongation. *Science* **289**, 619-625 (2000).

44 Cheetham, G. M. & Steitz, T. A. Structure of a transcribing T7 RNA polymerase initiation complex. *Science* **286**, 2305-2309 (1999).

45 Durniak, K. J., Bailey, S. & Steitz, T. A. The structure of a transcribing T7 RNA polymerase in transition from initiation to elongation. *Science* **322**, 553-557 (2008).

46 Yin, Y. W. & Steitz, T. A. The structural mechanism of translocation and helicase activity in T7 RNA polymerase. *Cell* **116**, 393-404 (2004).

47 Yin, Y. W. & Steitz, T. A. Structural basis for the transition from initiation to elongation transcription in T7 RNA polymerase. *Science* **298**, 1387-1395 (2002).

48 Yang, Z. *et al.* UCSF Chimera, MODELLER, and IMP: an integrated modeling system. *J Struct Biol* **179**, 269-278 (2012).